AMSI
AUSTRALIAN MATHEMATICAL SCIENCES INSTITUTE

National Collaboration in the Mathematical Sciences

Turing Patterns on Growing Domains

Sarah Armatys
Queensland University of Technology

February 2013

1 Introduction

In 1952, Alan Turing declared that certain systems of partial differential equations (PDEs) would produce what is now called *Turing instability* (Turing 1952). Turing instability is a phenomenon whereby if the system is slightly perturbed from its steady state and diffusion not allowed, then the system will fall back into the steady state. However, with diffusion, a unstable state, or pattern, is formed. Before Turing's conclusion, it was generally thought that diffusion only ever had a stabilising effect.

Turing instability has been suggested as a pattern forming mechanism for many applications (see 'Examples in literature' section). The initial derivations done by Turing were completed for applications that had a fixed spatial domain over the entire time of interest. However, in many contexts such as growing organisms, the domain grows over time. It is therefore worth investigating whether Turing instability still occurs in such problems.

1.1 Examples in literature

Many authors have studied pattern formation due to Turing instability. Various paradigm and real-life models have been analysed. Where real-life applications are studied, these most often are problems in organism growth at the start of life. Such patterns have included; teeth position in alligators (Kulesa et al. 1996), the location of mice limbs (Miura et al. 2006) or fish skin patterning (Kondo and Asai 1995). For such

Postal Address: 111 Barry Street
c/- The University of Melbourne
Victoria 3010 Australia

Email: enquiries@amsi.org.au
Phone: +61 3 8344 1777
Fax: +61 3 9349 4106
Web: www.amsi.org.au

applications, a growing domain, one or two dimensional model is normally used. Other applications include predator-prey distributions (Mukhopadhyay and Bhattacharyya 2006) and the distribution of chemical substances (Setayeshgar and Cross 1998).

In this report, we have chosen to analyse the paradigm Schnakenberg model in one spatial dimension (Schnakenberg 1979). This model describes the concentration of two substances u and v over time and is shown below in the non-dimensionalised form. The model arises from a three reaction, four substance system that includes the two substances of interest (u and v) as well as two external, non-depleting substances (Penny 2001).

$$\begin{aligned} \frac{\partial u}{\partial t} &= \gamma(a - u + u^2 v) + \frac{\partial^2 u}{\partial x^2}, \\ \frac{\partial v}{\partial t} &= \gamma(b - u^2 v) + d\frac{\partial^2 v}{\partial x^2}, \\ x \in [0, L], \quad t \in \mathbb{R}_+ \quad &\text{and} \quad \gamma, a, b, d \in \mathbb{R} \end{aligned} \tag{1}$$

Boundary conditions most often are no-flux (Neumann), occasionally Dirichlet. We have taken Neumann boundary conditions, therefore, to follow the literature.

1.2 Outline

In this report we derive the conditions for Turing instability for the Schnakenberg model on a one-dimensional fixed domain. After verfiying Turing instability occurs by solving the problem numerically, the issue of growing domains is considered. Several methods for including the domain growth in the system are compared, along with various growth functions and growth rates. The system is shown to display Turing instability in most cases.

2 Fixed domain

2.1 Conditions for Turing instability

Consider the following system of reaction-diffusion equations:

$$\begin{aligned} \frac{\partial u}{\partial t} &= F(u,v) + \frac{\partial^2 u}{\partial x^2} \\ \frac{\partial v}{\partial t} &= G(u,v) + d\frac{\partial^2 v}{\partial x^2} \\ d &\in \mathbb{R}\backslash\{1\} \end{aligned} \tag{2}$$

where F and G are in principle non-linear functions and d is the ratio of diffusivities of u and v. Let the vector $\boldsymbol{w}$ be the vector containing both solutions u and v, that is $\boldsymbol{w} = \begin{bmatrix} u \\ v \end{bmatrix}$. Assuming (u_0, v_0) is a steady state of (2) and linearising about this point, gives:

$$\boldsymbol{w_t} = \boldsymbol{J}\boldsymbol{w} + \boldsymbol{D}\boldsymbol{w_{xx}}, \;\; \boldsymbol{J} = \begin{bmatrix} F_u & F_v \\ G_u & G_v \end{bmatrix}_{(u_0,v_0)} \text{ and } \boldsymbol{D} = \begin{bmatrix} 1 & 0 \\ 0 & d \end{bmatrix}$$

Where F_u denotes the partial derivative of F with respect to u etc. For (2) to display Turing instability, it can be shown that four conditions must be met:

$$\begin{aligned} &\text{Condition 1: } F_u G_v - G_u F_v > 0 \\ &\text{Condition 2: } F_u + G_v < 0 \\ &\text{Condition 3: } dF_u + G_v > 0 \\ &\text{Condition 4: } (G_v + dF_u)^2 - 4d|\boldsymbol{J}| > 0 \end{aligned}$$

The derivation of these conditions is shown in Appendix A.

One may notice that the parameter d cannot be equal to 1 if conditions 2 and 3 are to be simultaneously satisfied. That is, the diffusivities of u and v cannot be equal, as we already noted.

2.2 Schnakenberg model

The steady state of the Schnakenberg model is found at:

$$u_0 = a + b \quad \text{and} \quad v_0 = \frac{b}{(a+b)^2}$$

As such, b must be positive and $a > -b$ for a physically realistic steady state. Further bounds on the parameters can be found by imposing the four conditions presented above. These bounds are:

$$d > 1, \quad b - a < (a+b)^3, \quad d(b-a) > (a+b)^3$$
$$\text{and} \quad \left(-(a+b)^2 + \frac{d(b-a)}{a+b}\right)^2 > 4d(a+b)^2$$

2.3 Numerical solutions

Using a forward difference in time, centred difference in space (FTCS) finite difference scheme, the concentrations of both substances over time were evaluated. All further models (see following sections) also used such a numerical scheme. Although using an implicit numerical scheme (for example, a backward difference approximation to the time derivative) would have ensured numerical stability no matter the mesh size used, an explicit scheme was chosen. This was because unlike an implicit scheme, an explicit scheme could easily deal with the non-linear and coupled nature of the system.

Two simulations done for a constant one-dimensional domain are given in Figure I below. The choice of parameters (a, b etc.) was made by randomly generating several choices for each parameter and then choosing a set of parameters such that the conditions given in 2.2 were satisfied. The plot on the right has a domain size four times that of the left. The initial disturbance was applied to u only, 10% along the domain. This disturbance was 10% of the steady state u value.

In both of these examples, the peaks in one substance correspond to the troughs in the other (only one substance is shown). For the plot on the left, the pattern that emerges has less peaks than that on the right. Both examples, however, have a sinusoidal shape of similar frequency for their end profiles (both of these frequencies are not the most unstable mode, but are close to it). Note, also, how the pattern does appear earlier near the initial disturbance point, but quickly spreads across the domain (this is more noticeable in the right plot).

3 Growing domain - methods

As stated earlier, the initial work done regarding Turing instability was all on fixed domains. This includes the derivation of the conditions for Turing instability done in

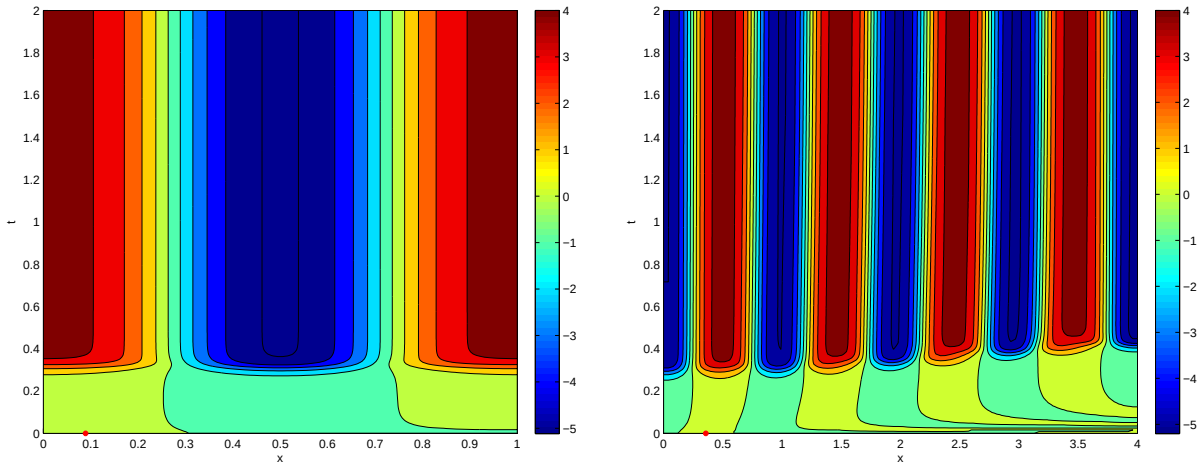

Figure I - difference from steady state value of u component of (1) for two different fixed domains. The system parameters are: a = -8.4, b = 12.43, d = 13.23, γ = 27.13. Left: domain [0,1], Right: domain [0,4].

this report. However, real-life applications often are on growing domains. We therefore wish to know whether Turing instability can still occur on such domains, and if so, what the patterns produced look like. It was decided then to use the Schnakenberg model (1) and analyse its behaviour on the domain $[0, L(t)]$, where $L(t)$ is the domain length at time t and $L(0) = 1$. Three different methods were devised to incorporate growth into the model. A description of each follows.

3.1 Rudimentary method

At first, a rudimentary method was used to simulate the growing domain. This method added node points in the spatial dimension as the domain grew. The timing of these additions depended on the growth function. However, it was soon realised that adding node points is not numerically stable. Also, when growth was fast or a long time was simulated, the large number of nodes needed made the computation expensive.

3.2 First growing method

To improve the method, a co-ordinate transform using the original equations was proposed. This transform mapped the domain from $[0, L(t)]$ to $[0, 1]$ for all t, where $L(t)$ was the length of the domain at time t. The transformed variables were $\hat{x} = \frac{x}{L}$ and $\hat{t} = t$ (see Landman, Pettet, and Newgreen 2003 for a similar transformation). As such, no node points needed to be added. This method was denoted as the 'first growing method'. Using the original governing equations (1), the new equations were derived using:

$$u_{xx} = \frac{u_{\hat{x}\hat{x}}}{L^2} \quad \text{and} \quad u_t = u_{\hat{t}} + u_{\hat{x}} \frac{-\hat{x}}{L} L_{\hat{t}}$$

resulting in:

$$\begin{aligned} u_{\hat{t}} &= \gamma(a - u + u^2 v) + \hat{x} \frac{L_{\hat{t}}}{L} u_{\hat{x}} + \frac{1}{L^2} u_{\hat{x}\hat{x}} \\ v_{\hat{t}} &= \gamma(b - u^2 v) + \hat{x} \frac{L_{\hat{t}}}{L} v_{\hat{x}} + d \frac{1}{L^2} v_{\hat{x}\hat{x}} \end{aligned} \tag{3}$$

To approximate the first derivative in space, a forward difference approximation was used. This was due to the fact that the coefficient in front of this term was always positive for a growing (that is, not shrinking) domain.

These equations assume that the isotropic growth of the domain does not give rise to any sort of advection. In other words, the expansion of the underlying substrate does not aid in the dispersion of substance u or v. An example of a physical system that may observe this principle is two gases in an expanding chamber. Since the gases are not 'attached' to the domain, the expanding chamber walls should not affect the gases.

3.3 Second growing method

Many interesting applications are not in a gaseous medium, however. Rather, the chemicals of interest are in a liquid or solid substrate and so the growth of the substrate will aid diffusion. As such, the first growing method cannot be used. Another method was then proposed for this situation (named the 'second growing method' in this report). The governing equations for this method were obtained from Crampin, Gaffney, and Maini 1999 and are derived from first principles using the ideas of mass-balance. The same co-ordinate transformation used earlier was then implemented.

The governing equations before and after co-ordinate transform are given below. Note that when the domain is fixed (that is, $L_t = 0$) the equations simplify to the original Schnakenberg equations.

$$\text{Before:} \qquad \begin{aligned} \frac{\partial u}{\partial t} + \frac{L_t}{L}\left(u + x\frac{\partial u}{\partial x}\right) &= \frac{\partial^2 u}{\partial x^2} + \gamma(a - u + u^2 v) \\ \frac{\partial v}{\partial t} + \frac{L_t}{L}\left(v + x\frac{\partial v}{\partial x}\right) &= d\frac{\partial^2 v}{\partial x^2} + \gamma(b - u^2 v) \end{aligned}$$

$$\text{After:} \qquad \begin{aligned} u_{\hat{t}} &= \gamma(a - u + u^2 v) - u\frac{L_{\hat{t}}}{L} + \frac{1}{L^2}u_{\hat{x}\hat{x}} \\ v_{\hat{t}} &= \gamma(b - u^2 v) - v\frac{L_{\hat{t}}}{L} + d\frac{1}{L^2}v_{\hat{x}\hat{x}} \end{aligned} \tag{4}$$

It can be seen that (3) and (4) differ in only one term. For both methods, this term is proportional to $\frac{L_{\hat{t}}}{L}$. As such, when the domain grows slowly (and hence $\frac{L_{\hat{t}}}{L}$ is small), the term will become negligible and the two methods should give similar results.

4 Numerical Comparison

4.1 Methods

We simulated all three methods and compared their results, as shown in Figure II. All plots are for the final profile (i.e. the concentration at the last time step). Like earlier, an initial displacement of 10% of the steady state u value was applied to u at the position specified (no disturbance was made to v). Note that with different growing functions, the final length reached after a common time period is not necessarily the same. However, since we used a small growth rate in the following three examples, the final length was similar for all three growth functions. These growth functions are

given below (r is the rate parameter and $L(0) = 1$ for all functions):

$$\text{Linear:} \quad L(t) = 1 + rt, \quad \frac{L_{\hat{t}}}{L(\hat{t})} = \frac{r}{1 + r\hat{t}}$$

$$\text{Exponential:} \quad L(t) = e^{rt}, \quad \frac{L_{\hat{t}}}{L(\hat{t})} = r$$

$$\text{Logarithmic:} \quad L(t) = 1 + \ln(1 + rt), \quad \frac{L_{\hat{t}}}{L(\hat{t})} = \frac{r}{(1 + r\hat{t})(1 + ln(1 + r\hat{t}))}$$

For most of the examples in literature, growth is approximated as a slow, exponentially growing process (for example, Crampin, Gaffney, and Maini 1999). The assumption of exponential growth simplifies the $\frac{L_{\hat{t}}}{L(t)}$ ratio to the constant growth rate parameter, as displayed above. The further assumption of slow growth means that a suitable approximation to the governing equations can be made by omitting the whole $\frac{L_{\hat{t}}}{L(t)}$ term. As such, the first and second growing methods become identical.

Although three growth functions are shown above, only plots for the linear growth function are shown in Figure II. This was because the three growth functions produced visually identical results. Further investigation into the effect of differing growth functions is made in the next section.

For all plots in Figure II, the rudimentary and second growing method produce similar results. It is not known why the rudimentary method is approximating the second growing method and not the first. One possible explanation may be the effect of boundary conditions - further investigation could be done on this issue. The first growing method, meanwhile, gave somewhat similar curves to the two others for larger growth rates and very similar curves for small growth rates (as expected). Taking the difference of the two curves (not shown), it can be seen that there is still a small systematic difference between the two methods.

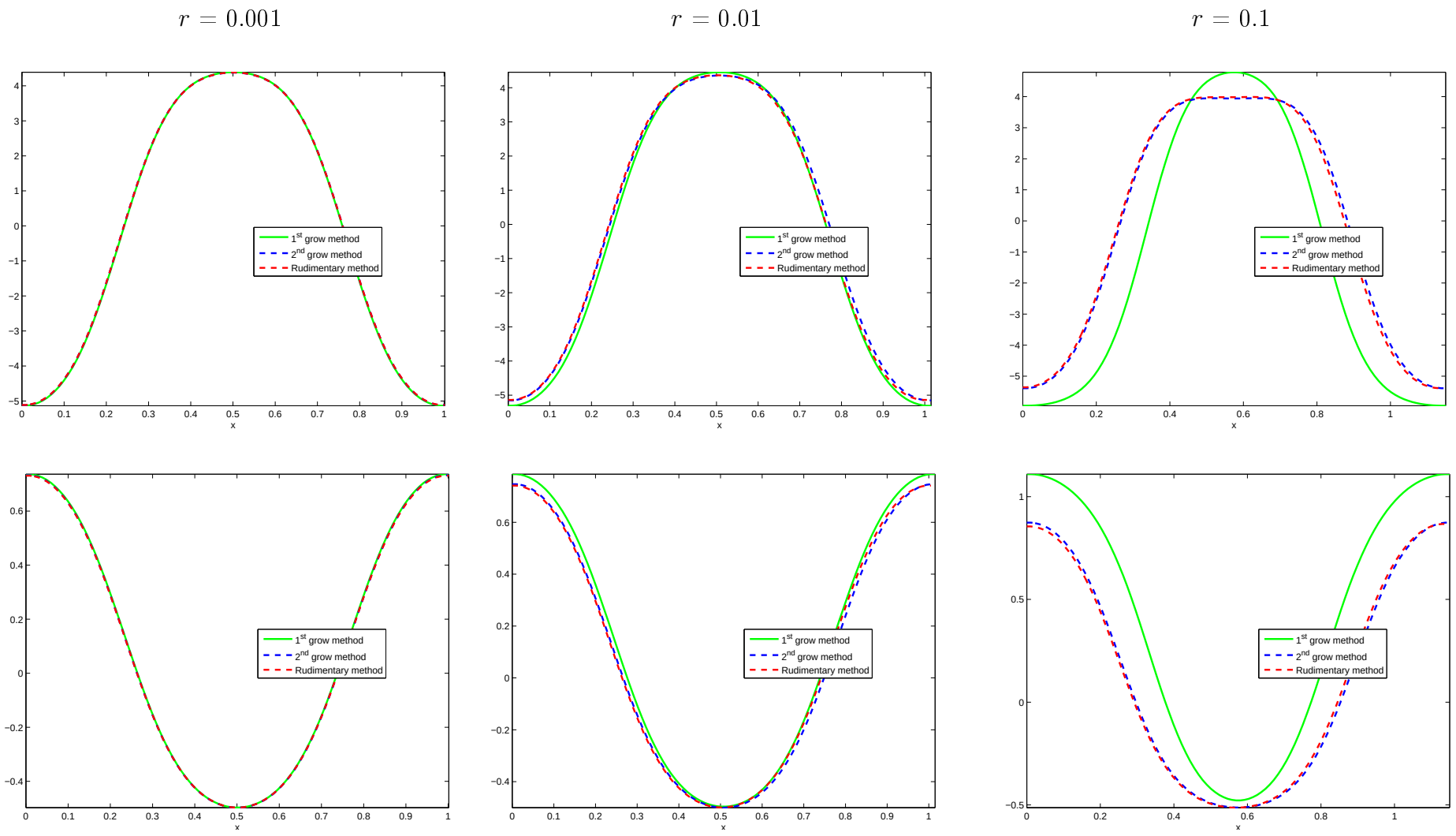

Figure II - difference from steady state value of u component of (1) for growing domains. The system parameters are: a = -8.4, b = 12.43, d = 13.23, γ = 27.13, 1.5 time units, initial displacement at 0.3, linear growth. First row is u, second row is v.

4.2 Growth functions

For most applications, the second growing method will be the method that best models the situation and is the most numerically stable of all of the three methods presented. As such, further investigation using this method was completed for even larger growth rate parameters. Larger growth rate parameters were chosen so that a greater distinction between the different growth functions could be seen.

In the previous section, all three methods were run with the same growth rate parameter and so the domain length was not the same for all functions at the end of simulation. For large growth rate parameters, this means that the difference between the domain lengths can be quite large at the end of simulation. To better compare the growth functions, therefore, it was decided to make the r parameter different for each growth function. For all further examples in this section, this parameter was set so that at the end of the simulated time period, all growth functions reached the same domain length (see the left column of Figure III).

For the first row in Figure III, the different growth functions do not appear to have a large impact on the resulting concentration profile. However, this was not the case when the system was made to reach a larger final domain length in the same amount of time. For this to happen, the value of r for each growth function was increased. This is shown in the second row of Figure III and Figure IV. A very interesting occurrence now happened - while the linear and exponential growth functions produced (different) patterns, the logarithmic failed to produce any sort of pattern. Instead, the concentration became equal over the domain while growing in time (i.e. not a steady state).

It is not shown here, but when the final domain length was increased further, the linear function too fell into an non-stable isotropic state. A further increase and all three functions produced no pattern. It is hypothesised that this order (logarithmic, linear, exponential) is due to the gradient of the domain growth function in the early stage of growth. As seen in Figure III, the order of decreasing initial domain growth gradient is the same as the order of failing pattern.

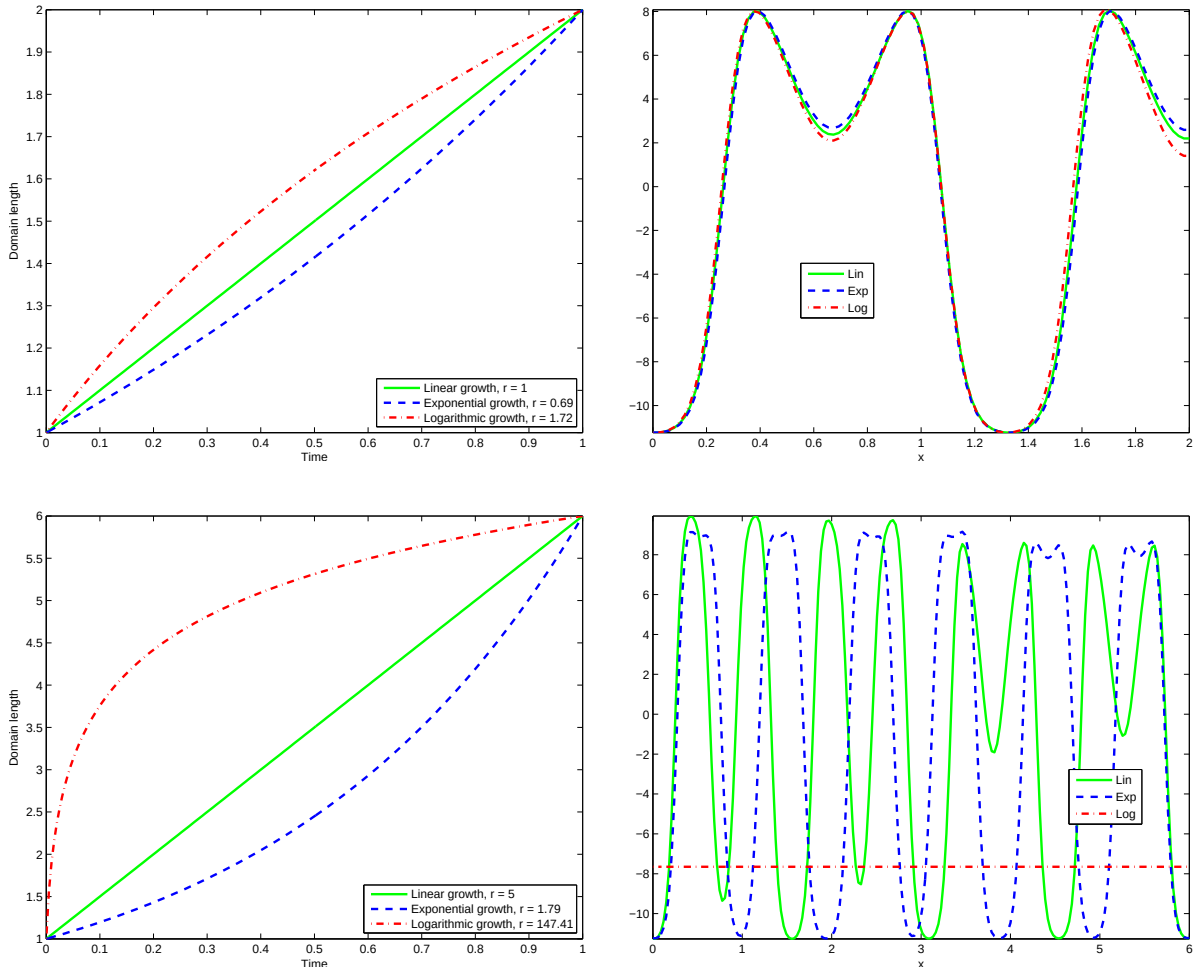

Figure III - fast growing domains. The system parameters are: a = -36.38, b = 43.6, d = 23.2, γ = 29.08, 1 time unit, initial displacement at 0.2. Left column: domain growth for each growth function, Right column: difference from steady state value of u at end of time period. First row: final length of 2, Second row: final length of 6.

Postal Address: 111 Barry Street
c/- The University of Melbourne
Victoria 3010 Australia

Email: enquiries@amsi.org.au
Phone: +61 3 8344 1777
Fax: +61 3 9349 4106
Web: www.amsi.org.au

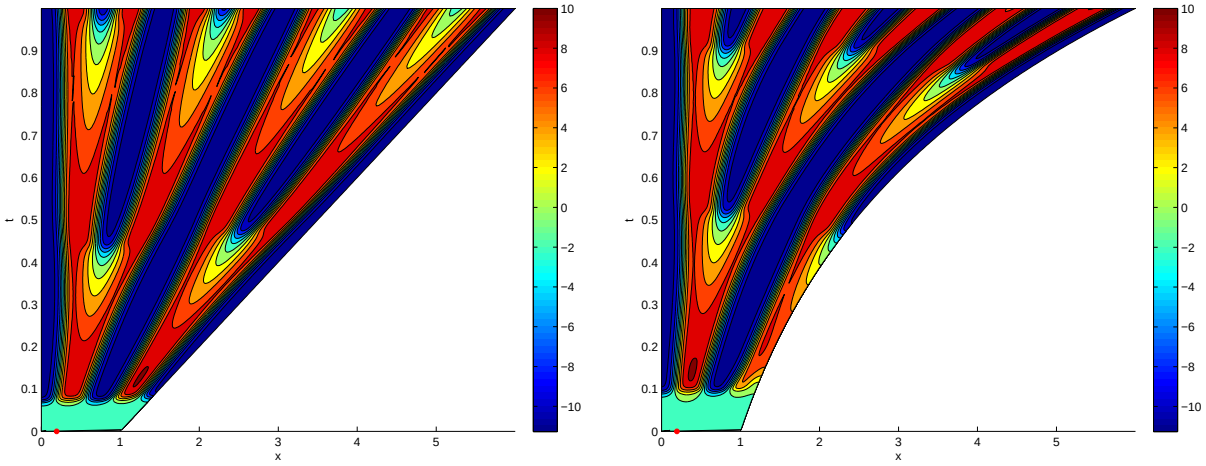

Figure IV - fast growing domains. The system parameters are: a = -36.38, b = 43.6, d = 23.2, γ = 29.08, 1 time unit, initial displacement at 0.2, final domain length of 6. Left: linear growth, Right: exponential growth

5 Conclusion

Turing instability on a growing domain was investigated. Three different methods for incorporating domain growth into the model were devised. Of these, the second growing method (which incorporated the effects of the growing domain on diffusion), was thought to model most real-life applications. For small growth rates, the three methods gave almost identical results (as expected). However, larger growth rates showed significant differences.

Three growth functions; linear, exponential and logarithmic, were also used, giving differing results. If the domain growth was too fast however, no pattern was produced. Further investigation into this matter could be made. For example, can we derive the growth rate at which patterning fails? Is this point a function of the model parameters (eg. a, b etc.)?

Also, an exponential function is often used for growth in literature, but it is surely not a realistic model for all domain growth. More research could be done on realistic growth functions/functions derived from empirical data.

6 Acknowledgments

I would like to thank very much my main supervisor Dr Petrus Van Heijster for his guidance and assistance in this project. My secondary supervisor A/Prof Scott McCue, also deserves thanks, especially for his help with the application process. Additionally, I would like to thank AMSI and CSIRO for their generous funding and for hosting the Big Day In.

Sarah Armatys received a 2012/13 AMSI Vacation Research Scholarship.

References

Crampin, Edmund J., Eamonn A. Gaffney, and Philip K. Maini (1999). "Reaction and diffusion on growing domains: Scenarios for robust pattern formation". In: *Bulletin of Mathematical Biology* 61 (6), pp. 1093–1120.

Kondo, Shigeru and Rihito Asai (1995). "A reaction–diffusion wave on the skin of marine angelfish Pomacanthus". In: *Nature* 376, pp. 765–768.

Kulesa, P.M. et al. (1996). "Modelling the spatial patterning of teeth primordia in the alligator". In: *Acta Biotheoretica* 44, pp. 153–164.

Landman, K.A., G.J. Pettet, and D.F. Newgreen (2003). "The Chemical Basis of Morphogenesis". In: *Bulletin of Mathematical Biology* 65, pp. 235–262.

Miura, Takashi et al. (2006). "Mixed–mode pattern in Doublefoot mutant mouse limb–Turing reaction–diffusion model on a growing domain during limb development". In: *Journal of Theoretical Biology* 240, pp. 562–573.

Mukhopadhyay, B. and R. Bhattacharyya (2006). "Modeling the Role of Diffusion Coefficients on Turing Instability in a Reaction–diffusion Prey–predator System". In: *Bulletin of Mathematical Biology* 68, pp. 293–313.

Penny, Melissa (2001). "Analysis of Reaction–Diffusion and Chemotatic Models on Growing Domains as a Mechanism for Pattern Formation". Honours Thesis. Queensland University of Technology.

Schnakenberg, J. (1979). "Simple chemical reaction systems with limit cycle behaviour". In: *Journal of Theoretical Biology* 81.3, pp. 389–400.

Setayeshgar, S. and M. C. Cross (1998). "Turing instability in a boundary–fed system". In: *Physical Review E* 58.4, pp. 4485–4500.

Turing, A. M. (1952). "Mathematical Models of Cell Colonization of Uniformly Growing Domains". In: *Proc. R. Soc. B.* 237.641, pp. 37–262.

A Deriving conditions for Turing instability on fixed domains

If λ_1, λ_2 are eigenvalues of J then $\lambda_1\lambda_2 = |\boldsymbol{J}|$ and $\lambda_1 + \lambda_2 = \mathrm{Tr}(\boldsymbol{J})$. For (u_0, v_0) to be stable without diffusion, both eigenvalues need to be negative. As such, two conditions on the Jacobian's entries can be derived;

$$\begin{aligned} |\boldsymbol{J}| > 0 \quad &\Rightarrow \quad F_u G_v - G_u F_v > 0 \\ \mathrm{Tr}(\boldsymbol{J}) < 0 \quad &\Rightarrow \quad F_u + G_v < 0 \end{aligned}$$

To find the conditions that ensure an unstable state is obtained with diffusion, first assume that $\boldsymbol{w}$ is of the form below.

$$\begin{aligned} \boldsymbol{w} &= \boldsymbol{w_0} e^{ikx} e^{\lambda t} \\ \text{and so} \quad \boldsymbol{w_{xx}} &= \boldsymbol{w_0}(ik)^2 e^{ikx} e^{\lambda t} = -k^2 \boldsymbol{w} \end{aligned}$$

The assumption of $\boldsymbol{w}$'s form holds for an unbounded domain. For a bounded domain with Neumann boundary conditions, we need to assume that $\boldsymbol{w} = \boldsymbol{w_0}\cos(ikx)e^{\lambda t}$. Of course, this alternate form still gives the same form for $\boldsymbol{w_{xx}}$.

Substituting for $\boldsymbol{w_{xx}}$ and letting $\boldsymbol{w_t} = 0$ gives:

$$0 = (\boldsymbol{J} - k^2\boldsymbol{D})\boldsymbol{w} = |\boldsymbol{J} - k^2\boldsymbol{D}|$$

Let $\boldsymbol{A} = \boldsymbol{J} - k^2\boldsymbol{D}$. As such, the trace of $\boldsymbol{A}$ is:

$$\mathrm{Tr}(\boldsymbol{A}) = F_u - k^2 + G_v - k^2 d = F_u + G_v - k^2(1+d)$$

Recall that as a ratio of diffusivities, d cannot be negative. Also, $F_u + G_v < 0$ by condition 1. Hence, $\mathrm{Tr}(\boldsymbol{A}) < 0$. As $\mathrm{Tr}(\boldsymbol{A}) = \lambda_a + \lambda_b$ (where λ_a, λ_b are the eigenvalues of A), at least one eigenvalue must therefore be negative. However, if both are negative, then a stable state is reached. The eigenvalues must then be of opposite signs and the determinate of A negative:

$$\begin{aligned} |\boldsymbol{A}| = \lambda_a\lambda_b < 0 \\ (F_u - k^2)(G_v - k^2 d) - G_u F_v < 0 \end{aligned}$$

$$F_u G_v - G_u F_v - k^2(G_v + dF_u) + k^4 d < 0$$
$$|\boldsymbol{J}| - k^2(G_v + dF_u) + k^4 d < 0 \tag{5}$$

Recall that $|\boldsymbol{J}| > 0$. Thus $G_v + dF_u > 0$ for (5) to hold. This is condition 3.

Letting $K = k^2$, the left-hand-side of equation 5 becomes a quadratic in K:

$$|\boldsymbol{J}| - K(G_v + dF_u) + K^2 d < 0$$

To ensure a real K (and hence k), then the following must be true:

$$(G_v + dF_u)^2 - 4d|\boldsymbol{J}| > 0$$

which is condition 4.